A Contactless and Fine-grained Sleep Monitoring System Leveraging WiFi Channel Response

Yu Gu*, Chenyu Zhang*, Yantong Wang*, Zhi Liu†, Yusheng Ji‡ and Jie Li§
* School of Computer and Information, Hefei University of Technology, China
† Department of Mathematical and Systems Engineering, Shizuoka University, Japan
‡ National Institute of Informatics, Japan
§ Shanghai Jiao Tong University, China.

***Abstract*—How can we effectively log a fine-grained sleep record consisting of still postures and in-place motions for the sleep disorder diagnosis without any specialized hardware? Existing sensor-based or vision-based solutions are either obstructive to use or rely on particular devices. This paper introduces SleepGuardian, a Radio Frequency (RF) based sleep monitoring system leveraging only omnipresent WiFi signals to provide a silent (unobtrusive and free of privacy concerns) yet loyal (fine-grained and reliable) logging service. The key to SleepGuardian is to model the energy feature of wireless channel as a Gaussian Mixture Model (GMM) to adaptively recognize motions happened during sleep. We prototype SleepGuardian with off-the-shelf WiFi devices and evaluate it in an office. Experimental results over 11 subjects with several artificial and real periods of sleep demonstrate that SleepGuardian is *effective* since it achieves 100% overall accuracy (ACC), 0% false negative rate (FNR) and 0.64 s mean absolute error (MAE) on average. Considering that SleepGuardian is compatible with existing WiFi infrastructure, it constitutes a low-cost yet promising solution for sleep monitoring.**

I. Introduction

Sleep is crucial for the wellness of human being. During sleep, human body remains in an anabolic state to restore both the muscular and nervous systems vital to the body and cognitive function. Individuals with sleep time deviating from the population norm are at risks of various sleep disorders like SDB, SBD, RLS, PLMS [1]. Some of them are serious enough to interfere with normal physical, mental, social and emotional functioning, especially hazardous for the elderly.

Sleep disorders are shown to be diagnosable via a fine-grained sleep history log represented in terms of *still postures* and *in-place motions* [2]. The log contains information like timing and regularity of bedtime, onset of sleep, nighttime awakenings, time of waking up in the mornings, daytime naps, and daytime sleepiness, etc. However, it is very challenging to acquire such long-term logs since manual collection is quite time-consuming and labor-intensive.

Actigraphy (ACT) has been accepted as a valid tool for this sleep history logging problem by the American Sleep Disorders Association (ASDA) at 1995 [3]–[5]. It refers to methods using wristband-like devices to monitor and collect data generated by body movements. Several such commercial products are already available on the open market such as Mi Band [6] and Fitbit [7]. Actigraphy is often considered to be effective but sometimes obtrusive for disturbing sleep. Some recent research try to improve its usability by attaching sensors to the objects where people lie on rather than the people themselves, e.g., force sensing resistor sensors on the staves of the bed [8] or polyvinylidene fluoride (PVDF) film sensors on a mattress [9], raising the mobility and coverage issue at the same time. Other research like vision systems [10]–[13] could be contactless but still obstructive due to the coverage issue: illumination and line-of-sight (LOS) restrictions. Last but not least, the privacy issue cannot be overlooked.

To this end, we design SleepGuardian, a wireless channel data-driven sleep monitoring system leveraging commodity WiFi infrastructure only. Compared to its sensor and vision based rivals, SleepGuardian has three advantages. Firstly, it does not relies on specialized hardware since the low-cost WiFi infrastructure is pervasive nowadays. Secondly, it is robust since characterizing the channel response as the Gaussian Mixture Model waives the site-dependent calibrations and target-dependent training. Lastly, it is contactless and free of privacy concerns since the WiFi signal is transparent for users.

We prototype SleepGuardian with low-cost, off-the-shelf WiFi devices and evaluate its performance in a 7×10 m^2 office. We recruit 11 subjects and ask them to perform a controlled 2-minute behavior consisting of in-place motions and still postures 5 times. Numerical results suggest that SleepGuardian is *1) effective* since it achieves 100% ACC, 0% FNR and 0.64 s MAE on average, *2) robust* since the impact of external circumstances like site, target, illumination, and line-of-sight is limited, and *3) unobtrusive* since no subject reports privacy or comfort complaints as in the vision-based and sensor-based rivals.

This paper contributes to the current research on sleep monitoring from the following aspects:

- We characterize channel response of still sleeping postures with a Gaussian Mixture Model, which enables us to adaptively distinguish in-place motions (foreground) from still postures (background) without site-dependent calibrations or target-dependent training.
- We prototype SleepGuardian with commodity WiFi devices. Evaluation of SleepGuardian in real environments demonstrate its effectiveness and robustness.

The rest of this paper is organized as follows: our system design has been described in Section II. We prototype Sleep-

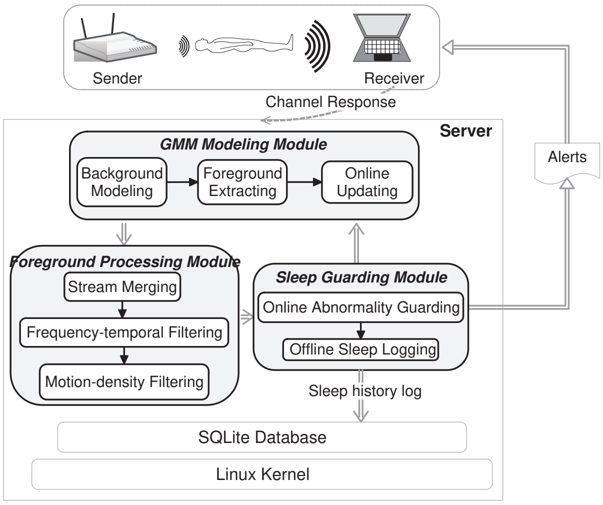

Fig. 1. System overview of SleepGuardian.

Guardian and evaluate its performance in Section III. Finally, we conclude our work and outline future work in Section IV.

II. System Design

In this section, we first give an overview of our SleepGuardian and then present its detailed designs following the CSI data flow.

A. System Overview

Fig. 1 shows the system architecture of SleepGuardian. The WiFi signal periodically emitted by the sender flows through the target subject and reaches the receiver. The relative position and distance between Tx and Rx can significantly influence the performance of SleepGuardian. The deployment of antennas is shown in Fig. 3. The attenuated signal described by channel response contains rich and detailed descriptions of the subject like still postures and in-place motions via the multi-path and fading effects. To retrieve fine-grained sleeping information from the signal, the receiver leverages three modules to process CSI data (channel response), i.e., GMM modeling module (aims to extract foreground from background), foreground processing module (targets on removing counterfeit foreground) and sleep guarding module (records the duration of different still postures, and the start time, duration and intensity of in-place motions).

B. GMM Modeling Module

(0) CSI Visualizing. We partition the stream into consecutive windows with length T, containing N samples for each subcarrier [14]. Then each frame contains $M \times N$ pixels, where M is the number of subcarriers. The color of each pixel $P_{m,n}$ is determined by mapping its amplitude value to a predefined colormap.

Fig. 2 is an example. The experimental settings remain the same as in the preliminary experiment. Fig. 2(a) represents the visualized raw CSI trace on antenna #3, where the rollovers (vertical lines crossing most of subcarriers) are vivid.

(1) Background Modeling. Within one frame, each pixel is modeled by a mixture of K Gaussian distributions. The probability that a certain pixel has a value (dBm) of x_t at time t can be written as,

$$p(x_t) = \sum_{i=1}^{K} w_{i,t}\eta(x_t, \mu_{i,t}, \Sigma_{i,t}) \quad (1)$$

where $w_{i,t}$, $\mu_{i,t}$ and $\Sigma_{i,t}$ are the weight, the mean value and the covariance of the i-th Gaussian component at time t, respectively.

The K distributions are ordered by the fitness value $\frac{w_{i,t}}{\sigma_{i,t}}$, and then the first B distributions are chosen as the background where B is derived as follows,

$$B = \arg\min_b (\sum_{i=1}^{b} w_{i,t} > P) \quad (2)$$

Where the threshold P is the minimum fraction of the background model. We set P to 0.3 in Sleepy.

(2) Foreground Extracting. If an incoming pixel does not fit in the background model, it is likely to be the foreground. More specially, if this pixel is more than 2.5 standard deviations away from any of the B distributions in the background model, it is marked as the foreground, i.e.,

$$|x_t - \mu_{i,t}| \geq 2.5 \cdot \sigma_{i,t} \quad (3)$$

Fig. 2(b) visualizes the CSI frames after extracting foregrounds of antenna #3, where rollovers have been roughly captured with some counterfeit foregrounds that are not caused by motions.

(3) Online Updating. To accurately distinguish foregrounds from changing backgounds, online updating is essential:

The initial weight and variance of K distributions are set to $\frac{1}{K}$ and 1.5, respectively.

If none of the K distributions match the current pixel, the model is updated by replacing the distribution with **the least fitness value** with a new Gaussian distribution whose mean is set to the value of current pixel while using an initial weight ($\frac{1}{K}$) and variance (1.5). Then, we normalize the weight of all K distributions.

Otherwise, we update the weight of all K distributions as follows,

$$w_{i,t} = (1-\alpha)w_{i,t-1} + \alpha M_{i,t} \quad (4)$$

where α is a pre-defined learning rate. $M_{i,t}$ will be 1 if i is the first match distribution otherwise 0.

Then, we normalize the weight of all K distributions.

Lastly, we update the first matched distribution as follows,

$$\mu_{i,t} = (1-\rho)\mu_{i,t-1} + \rho x_t \quad (5)$$

$$\sigma^2_{i,t} = (1-\rho)\sigma^2_{i,t-1} + \rho(x_t - \mu_{i,t})^2 \quad (6)$$

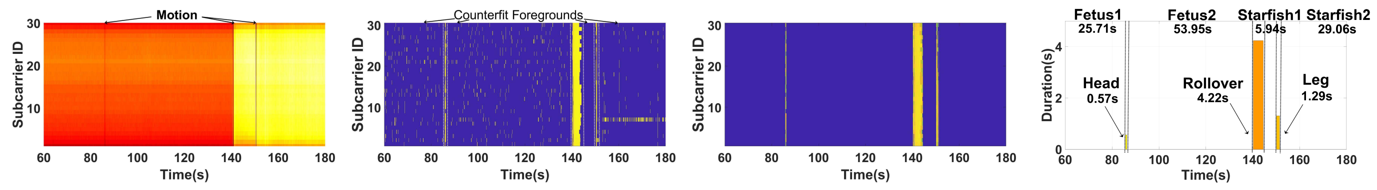

(a) Raw CSI visualizing: antenna #3 (b) After GMM modeling module: antenna #3 (c) After foreground processing module (d) After sleep guarding module

Fig. 2. The 2-minute fragment: (a) Initialization: the raw CSI trace on antenna #3 has been visualized with highlighted motions; (b) After GMM modeling module: real and counterfeit foreground co-exist; (c) After foreground processing module: counterfeit foregrounds have been cleared; (d) After sleep guarding module: a sleep record has been generated.

where $\rho = \frac{\alpha}{w_{i,t}}$ is a temporary parameter and α is set to 0.01 in Sleepy.

The online updating endues Sleepy with the ability to adapt to background changing without extra calibrations or target-dependent training.

Fig. 2(b) visualizes the CSI data after the GMM modeling module on antenna #3. The blue background represents still postures (fetus and starfish), while the foreground has been marked in yellow. Three real motions appear vividly on the graph, but there are still scattered counterfeit foregrounds. In the next module, we will try to remove them.

C. Foreground Processing Module

This module processes foregrounds in two steps, i.e., enhancing the real foregrounds via stream merging and removing the counterfeit ones via two filters.

(4) Stream Merging. The preliminary suggests that the motion of different body parts has varying degrees of impact on different antennas. Therefore, we should merge the CSI data in all three antennas to enhance the impact of motions following a simple rule: one pixel marked as a foreground on any antenna remains so in the merged frame. Otherwise, it is a background.

Stream merging enhances the real foregrounds but also brings more counterfeit ones, which are likely caused by two reasons: device interference and human interference. The former is usually caused by system glitches or other wireless devices competing for the same channel, while the latter is caused by nearby human beings.

(5) Frequency-temporal Filtering. This filter deals with device interference. It leverages a basic fact: human motions usually lasts for a period of time, leading to the temporal correlations of foregrounds. Also, human motion changing the signal propagation path usually affects multiple subcarriers, resulting in the frequency correlations of foregrounds. However, a device interference is brief, random and scattered. Therefore, any foreground segment at time t meeting either of the following criteria will be marked as background,

- It lasts less than τ seconds.
- It affects less than p of all subcarriers.

Where τ and p are set to 0.1 and 70% in SleepGuardian, respectively.

(6) Motion Density Filtering. This filter handles human interference. It is built on a general investigation: a non-line-of-sight (NLOS) human motion usually leaves a much lighter impact on channel response than its LOS kind. Therefore, we use a sliding window of 0.5 s length and evaluate the density of foregrounds within the window. If its density is lower than d, all foregrounds within the current window will be marked as background. d is set to 0.4 in SleepGuardian.

Fig. 2(d) visualizes the CSI frames after the foreground processing module, where the vertical lines representing motions have been enhanced, while the counterfeit foregrounds have been thoroughly removed.

D. Sleep Guarding Module

This module provides two services based on the filtered foreground and background, i.e., offline sleep logging and online abnormality guarding:

(7) Offline Sleep Logging. This service estimates the duration of different sleep postures and the start time, duration and intensity of motions, based on which a fine-grained sleep log is generated including timing and regularity of bedtime, onset of sleep, nighttime awakenings, time of waking up in the mornings, daytime naps, and daytime sleepiness.

Fig. 2(d) demonstrates such a record of the 2-minute fragment: fetus for 25.71 s with a head movement lasting for 0.57 s, fetus for 2 s, rollover for 4.22 s, starfish for 35 s with a leg movement lasting for 1.29 s .

(8) Online Abnormality Guarding. This service keeps guarding the subject for any abnormal behaviors like intensive body twitches from a nightmare, a sudden seizure attack or falling off the bed. Once an abnormality happens, it will automatically warn the designated contacts like a nearby emergency room or a closeby relative.

The abnormality is application-dependent. For instance, an abnormality of an infant could be an unusually high frequency of motions, implying that s/he is awake feeling uncomfortable on bed and the parents should be warned. For a person having a history of seizure, the abnormality could be a series of periodic motions lasting for a few minutes.

In our prototype, we set a simplified condition to trigger the warning: *intensity of a motion exceeds certain threshold*. Because the intensity of normal motions like body adjustments and rollovers is generally bounded in a small range according

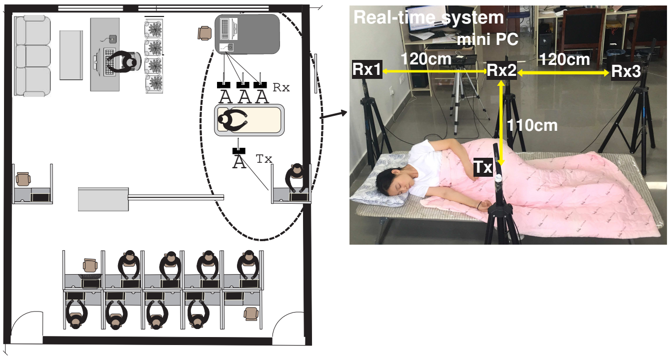

Fig. 3. Our testbed in a $7 \times 10m^2$ office: 1×3 data streams on the 5 GHz channel processed by a miniPC (2.16GHz CPU, 4GB RAM and 240GB SSD) mounted with an Intel 5300 NIC.

TABLE I

THE RESULTS FROM 2-MINUTE CONTROLLED CASE: THE SLEEPGUARDIAN ACHIEVES 97% ACC, 0.05% FNR AND 0.87 S MAE ON AVERAGE. EVERY TESTER PERFORMS A CONTROLLED 2-MINUTE BEHAVIOR CONSISTING OF IN-PLACE MOTIONS AND STILL POSTURES 5 TIMES.

TESTER IDENTIFIER	ACC	FNR (%)	MAE (s)
01 (F)	1.00	0.00	0.91
02 (M)	1.00	0.00	0.94
03 (M)	1.00	0.00	0.72
04 (F)	1.00	0.17	0.60
05 (F)	1.00	0.17	1.10
06 (M)	1.00	0.00	0.54
07 (M)	1.00	0.17	0.60
08 (F)	1.00	0.00	0.61
09 (M)	1.00	0.00	0.75
0A (M)	0.66	0.00	1.48
0B (F)	1.00	0.00	1.33
AVERAGE	0.97	0.05	0.87

to our empirical studies, while a sudden and intensive motion usually means an accident.

III. Performance Evaluation

This section systematically evaluates the performance of SleepGuardian through 2-minute Controlled Case and 1-hour Real Sleep.

A. Evaluation Setup

The prototype consists of a commodity TP-LINK router (TP-link TL-WR845N) under 802.11b (5 GHz) and a mini PC (2.16GHz CPU, 4GB RAM and 240GB SSD) mounted with an Intel 5300 NIC as the receiver. The layout and the deployment of our prototype are shown in Fig. 3. Moreover, the packet delivery frequency at the sender is set to 330 Hz.

We recruit 11 volunteers to join our evaluation, including 5 females and 6 males. We ask them to perform a 2-minute controlled behavior consisting six motion sequences for each sequence we define contain several brief and continuous in-place motions, and a long time real sleep which was recorded by a camera (Logic C525) at the same time. The camera enables us to compare the results we get from our SleepGuardian with identification outcomes extracted from the recording videos and thus we could count ACC, FNR and MAE to further evaluate the effectiveness of our final system in usual environments. The aforementioned experiments are tested in a $7 \times 10\ m^2$ office.

Next, we assess the performance of SleepGuardian and make quantitative and qualitative analysis of the experimental results. Besides, some inspiring observations are reported for future work.

B. 2-minute Controlled Case

We ask 11 subjects to perform six predefined motion sequences 5 times in an office. Each motion sequence consists of several continuous short in-place motions. After that, we collect the CSI data from the receiver and invoke GMM modeling module and foreground processing module sequentially. Because the number of motion sequence is predetermined, we could sum up three indicators, i.e., overall accuracy (ACC), false negative rate (FNR) and mean absolute error (MAE). Finally, we calculate the average outcomes of those three indicators, respectively. The results are shown in Table. I. The SleepGuardian achieves 97% ACC, 0.05% FNR and 0.87 s MAE on average.

Intuitively, the actions we human beings do during real sleep are unintentional and irregular. Even if the statistical results are encouraging, one more evidence needs further investigation, that is the validity of our system in real sleep case.

Next, we will dig deeper through 1-hour real sleep case for more comprehensive coverage evaluation.

C. 1-hour Real Sleep

In this part, we ask 11 participants to take a real 1-hour nap with a camera recording in an office. To help them get to sleep easily and sleep soundly, we let each participator to sleep on their own pillow. Moreover, we turn off all lights and close the curtain to ensure a cozy environment.

We follow the same way as in the 2-minute controlled case to handle the CSI data collected from the receiver. The corresponding colormaps are shown in Fig. 4, which demonstrates the effectiveness of our foreground processing module which almost removes all fake backgrounds which may be caused by device interference or nearby human activities. Last but not least, we visualize the motion components by their duration length in Fig. 4(d). Besides, we manually count the number of motions and its approximate time of occurrence from the recording videos. Finally, we calculate three indicators from the aforementioned statistical results. The SleepGuardian achieves 100% ACC, 0% FNR and 0.64 s MAE on average. The results are better than previous 2-minute controlled case, which seems that SleepGuardian is more suitable for motion detection of real scenes.

Also, there is something interesting we have noticed. Fig. 4(d) shows that our system could accurately capture motions even if they are pretty brief. However, trivial motions are usually useless to diagnosing intention. This phenomenon proves the accuracy and fine-grained sensitivity of SleepGuardian indirectly. From the above observations, it inspires us to build

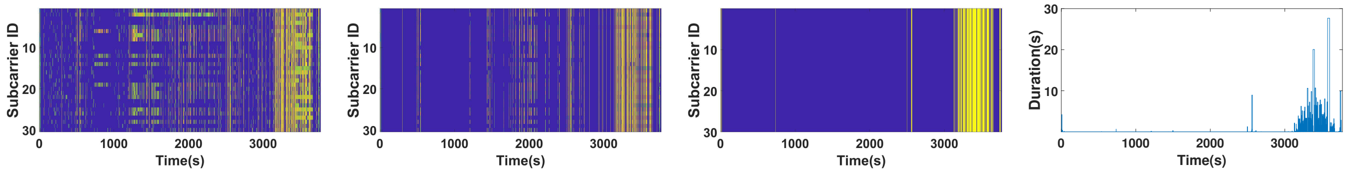

(a) After GMM modeling module (b) After frequency-temporal filtering (c) After motion density filtering (d) Motion component analysis by duration time

Fig. 4. The 1-hour real sleep fragment: (a) After GMM modeling module: real and counterfeit foreground coexist; (b) After frequency-temporal filtering: deals with the device interference; (c) After motion density filtering: handles the human interference; (d) Motion component analysis by duration time.

an application-level product which detects not the quality of sleep but whether the lying person is alive or not.

IV. Conclusion and Future Work

In this paper, we present SleepGuardian, a RF-based sleep monitoring system leveraging the off-the-shelf WiFi infrastructure. Unlike its vitals relying on sophisticated hardware or complicated training, it digs deeper into the channel characteristics and models the energy distribution over subcarriers as a Gaussian Mixture Model, which requires no calibrations or target-dependent training to detect normal or abnormal motions during sleep. SleepGuardian has been extensively evaluated in real environments from different perspectives and the results confirmed its reliability and efficiency. SleepGuardian can be seamlessly integrated into existing WiFi infrastructures, and thus constitutes a practical solution in the real world.

For the future work, one promising direction is to extend our current system for respiration and heartbeat, which allows us to provide a fine-grained monitoring service for more sleep disorders like sleep apnea or post-myocardial infarction. Another attempting extension is to extract certain patterns among different people to set up a model linking sleep postures and channel response. Last but not least, it is very crucial to extend SleepGuardian to handle more than one sleepers.

Acknowledgments

This work is sponsored by the National Natural Science Foundation of China (NSFC) under Grant No. 61772169, National Key Research and Development Program under Grant No.2018YFB0803403, and the Fundamental Research Funds for the Central Universities under No.JZ2018HGPA0272.

References

[1] N. C. Tan, M. S. Tan, S. W. Hwang, C. C. Teo, K. N. L. Zhi, Y. J. S. Jing, L. E. K. Yi, and C. H. How, "Sleep time and pattern of adult individuals in primary care in an asian urbanized community," *Medicine*, vol. 95, no. 35, p. e4749, 2016.

[2] A. Seelye, N. Mattek, D. Howieson, T. Riley, K. Wild, and J. Kaye, "The impact of sleep on neuropsychological performance in cognitively intact older adults using a novel in-home sensor-based sleep assessment approach." *Clinical Neuropsychologist*, vol. 29, no. 1, pp. 53–66, 2015.

[3] A. Sadeh, P. J. Hauri, D. F. Kripke, and P. Lavie, "The role of actigraphy in the evaluation of sleep disorders." *Sleep*, vol. 18, no. 4, pp. 288–302, 1995.

[4] A. S. D. Association, "Practice parameters for the use of actigraphy in the clinical assessment of sleep disorders." *Sleep*, vol. 18, no. 4, pp. 285–287, 1995.

[5] A. Domingues, T. Paiva, and J. M. Sanches, "Sleep and wakefulness state detection in nocturnal actigraphy based on movement information," *IEEE Transactions on Biomedical Engineering*, vol. 61, no. 2, pp. 426–434, 2014.

[6] "Mi band," Website, 2016, http://www.mi.com/en/miband2/.

[7] "Fitbit," Website, 2016, http://www.fitbit.com.

[8] P. Barsocchi, M. Bianchini, A. Crivello, D. L. Rosa, F. Palumbo, and F. Scarselli, "An unobtrusive sleep monitoring system for the human sleep behaviour understanding," in *IEEE International Conference on Cognitive Infocommunications*, Oct 2017.

[9] W. J. Da, H. H. Su, H. N. Yoon, Y. J. Lee, D. U. Jeong, and K. S. Park, "Nocturnal awakening and sleep efficiency estimation using unobtrusively measured ballistocardiogram." *IEEE transactions on biomedical engineering*, vol. 61, no. 1, pp. 131–8, 2014.

[10] C. W. Wang, A. Hunter, N. Gravill, and S. Matusiewicz, "Unconstrained video monitoring of breathing behavior and application to diagnosis of sleep apnea." *IEEE transactions on bio-medical engineering*, vol. 61, no. 2, pp. 396–404, 2013.

[11] M. H. Li, A. Yadollahi, and B. Taati, "Non-contact vision-based cardiopulmonary monitoring in different sleeping positions," *IEEE Journal of Biomedical & Health Informatics*, pp. 1–1, 2016.

[12] A. K. Abbas, K. Heimann, K. Jergus, T. Orlikowsky, and S. Leonhardt, "Neonatal non-contact respiratory monitoring based on real-time infrared thermography," *BioMedical Engineering OnLine*, vol. 10, no. 1, p. 93, 2011.

[13] J. Fei, I. Pavlidis, and J. Murthy, "Thermal vision for sleep apnea monitoring." in *Medical Image Computing & Computer-assisted Intervention: Miccai International Conference on Medical Image Computing & Computer-assisted Intervention*, 2009, pp. 1084–91.

[14] X. Zheng, J. Wang, L. Shangguan, Z. Zhou, and Y. Liu, "Smokey: Ubiquitous smoking detection with commercial wifi infrastructures," in *Proc. of IEEE INFOCOM 2016*, Hong Kong, April 2015, pp. 17–18.